Pharm Res (2013) 30:1536–1552
DOI 10.1007/s11095-013-0991-x

RESEARCH PAPER

A Physiologically Based Pharmacokinetic Model for Strontium Exposure in Rat

Henry Pertinez • Marylore Chenel • Leon Aarons

Received: 8 October 2012 / Accepted: 22 January 2013 / Published online: 30 March 2013

ABSTRACT

Purpose To develop a physiologically based pharmacokinetic (PBPK) model to describe the disposition of Strontium—a bone seeking agent approved in 2004 (as its Ranelate salt) for treatment of osteoporosis in post-menopausal women.

Methods The model was developed using plasma and bone exposure data obtained from ovariectomised (OVX) female rats—a preclinical model for post-menopausal osteoporosis. The final PBPK model incorporated elements from literature models for bone seeking agents allowing for description of the heterogeneity of bone tissue and also for a physiological description of bone remodelling processes. The model was implemented in MATLAB in open and closed loop configurations, and fittings of the model to exposure data to estimate certain model parameters were carried out using non-linear regression, treating data with a naïve-pooled approach.

Results The PBPK model successfully described plasma and bone exposure of Strontium in OVX rats with parameter estimates and model behaviour in keeping with known aspects of the distribution and incorporation of Strontium into bone.

Conclusions The model describes Strontium exposure in a physiologically rationalized manner and has the potential for future uses in modelling the PK-PD of Strontium, and/or other bone seeking agents, and for scaling to model human Strontium bone exposure.

H. Pertinez (✉)
Department of Molecular and Clinical Pharmacology
The University of Liverpool, Block H, 1st Floor 70 Pembroke Place
Liverpool L60 3CE, UK
e-mail: henry.pertinez@liverpool.ac.uk

M. Chenel
Clinical Pharmacokinetic Department Institut de Recherches
Internationales Servier, Suresnes Cedex, France

L. Aarons
Centre for Applied Pharmacokinetic Research
School of Pharmacy and Pharmaceutical sciences
The University of Manchester, Manchester, UK

KEY WORDS bone-seeking agent · osteoporosis · ovariectomised · PBPK · post-menopausal

ABBREVIATIONS

Art-blood	Arterial Blood
A_x	Amount of Strontium in tissue compartment x (mg)
BFR	Total Bone Formation rate (L/h)
Cl_x	Clearance of Strontium from blood by compartment x (L/h)
C_x	Concentration of Strontium in tissue compartment x (mg/L) equal to A_x/V_x
FBFR	Fractional Bone Formation Rate
F_u	Fraction unbound of Strontium in blood
ka	1st order absorption rate constant for Strontium from gut depot into gut tissue (h^{-1})
K_{p-x}	Tissue to blood partition coefficient for tissue compartment x
PP	Poorly perfused tissues
Q_x	Blood flow to tissue compartment x (L/h)
STRONT	Dimensionless scaling factor for Intercompartmental clearance of Strontium from bone tissue surface to bone tissue matrix
Ven-blood	Mixed Venous blood
V_x	Volume of tissue compartment x (L)
WP	Well perfused tissues
xBFR	Bone Formation rate in bone tissue type x (cortical or trabecular).
xBRR	Bone Resorption rate in bone tissue type x (cortical or trabecular).
xRVAF	Intercompartmental clearance of Strontium from bone tissue x surface compartment into bone tissue x matrix compartment (cortical or trabecular).

INTRODUCTION

It was demonstrated as early as the 1950s that low to moderate doses of Strontium (orally, as its lactate salt) could be used as an aid to Calcium deposition in the bone (1) and that Strontium lactate could hence be used as a treatment for osteoporosis (2). These findings were largely overlooked for a number of years however as interest in Strontium biology focussed on the health effects of radioisotopes of Strontium (^{90}Sr in particular, derived from nuclear fallout, which essentially became synonymous during much of the 20th Century for all forms of Strontium). In more recent years however, the use of Strontium in treating osteoporosis has been re-evaluated; dosed as its Ranelate salt in *in-vivo* animal models (e.g., the ovariectomised, oestrogen deficient female rat which is an *in-vivo* preclinical model for osteoporosis (3)), Strontium was shown to reduce bone resorption and promote bone formation, and to improve the bone tissue quality (4–11). This effect has been confirmed *in-vitro* where Strontium Ranelate was shown to enhance osteoblast activity (12) and inhibit the activity of osteoclasts (13). Strontium is thought now therefore to be the first dual acting agent that is able to uncouple the processes of bone resorption and formation by both inhibiting osteoclasts and stimulating osteoblasts respectively. The efficacy of orally dosed Strontium Ranelate (2 g/day) in the treatment of osteoporosis has gone on to be demonstrated in a number of human clinical trials, including phase III studies (more than 6500 postmenopausal osteoporotic women treated) that have shown that strontium ranelate significantly decreases the risk to have a new vertebral or non-vertebral fracture (such as hip fracture) over 3 and 5 years of treatment in osteoporotic post-menopausal women. Strontium ranelate concomitantly increases lumbar and hip BMD and these increases have been shown to be predictive of a reduction in vertebral and hip fracture risks. (14–16).

Strontium Pharmacokinetic Disposition

The dominant feature of the pharmacokinetic (PK) disposition of Strontium is its nature as a bone seeking agent (a class of molecules that share a high affinity for bone tissue (17)). In the case of drugs such as the bisphosphonates or Strontium where bone is the site of action these distributional attributes can be a key advantage (17). Studies with intravenous (IV) radioStrontium have shown that Strontium distributes out from the blood very rapidly (18) and is largely deposited at bone tissue. At therapeutic doses, the distribution of Strontium in bone tissue tends to be mainly limited to adsorption to bone surface, with a smaller molar fraction being incorporated into the hydroxyapatite mineral structure of newly formed bone. Levels of deposition vary according to local bone structure, skeletal site and bone age—higher content being observed in newly formed bone (19). It has been speculated that the high bone surface concentrations achieved as a result of adsorption may enhance Strontium's pharmacological effect on bone remodelling as this is the key location of osteoblast and osteoclast activity (20). When treatment is removed, surface exchange leads to a rapid decline in Strontium blood levels (19). Strontium ranelate is moderately absorbed intestinally (21) with a mechanism of gastrointestinal absorption involving, like Calcium, passive diffusion as well as saturable active transport and facilitated diffusion. Renal excretion is its main route of elimination clearance (22–25).

Disposition and Pharmacokinetic Modelling of Bone Seeking Agents

The PK and pharmacodynamics (PD) of bone seeking agents are made more complex due to the heterogeneity of bone tissue with its physiologically distinct cortical and trabecular subtypes. Cortical bone with its denser, stiffer structure, lower porosity and less rich blood supply, will have very different dispositional characteristics compared to trabecular bone which has a richer blood supply, more porous, honeycomb-like structure and greater surface of contact with bone marrow. Furthermore, the two bone types account for different proportions of the overall skeleton; largely constant between species, these are 80% and 20% by volume for cortical and trabecular bone respectively (26). Bone seeking agents will as a result not be homogeneously distributed in bone across an organism's skeleton as a whole. In addition, not only is there likely to be uneven distribution between cortical and trabecular bone, but also within each bone tissue type there will be a distinct difference between the bone surface and the bone matrix. The bone surface is covered in the cells (osteoblasts, osteoclasts etc.) involved in bone remodelling, turnover and maintenance and is in close contact with the blood supply and hence able to exchange compounds relatively rapidly. The deeper bone matrix is more distant from the blood, permeated by inter-osteoclast canalicules and in the case of cortical bone haversian canals; compounds deposited here will generally undergo slower exchange over time. Bone deposition will also vary according to the rates of remodelling in bone tissue, with trabecular bone generally showing a higher bone tissue turnover than cortical (26), and some physiological locations showing more turnover than others. The physical properties of mineralised bone tissue (e.g., density) are essentially the same however in cortical and trabecular bone tissue—the two tissue subtypes being differentiated principally by the spatial organisation of the matrix, their blood supply etc.

Examples of the modelling of the PK of bone seeking agents cover the spectrum from empirical compartmental models through to more complex mechanistic approaches (17), with PK models of bone seeking agents that are able to provide rational insight into (and prediction of) bone disposition being of particular value as systematic samples of human bone tissue can only rarely be obtained.

Among the more physiologically based PK models for bone seeking agents are the models implemented by O'Flaherty *et al.* to describe the PK of bone seeking metal elements (27), this work being relevant as Strontium is an alkaline-earth metal element. There are various aspects of metals that set them apart in disposition from typical organic xenobiotics, metals for example are not metabolised into new entities in the same sense that organic molecules can be (although their oxidation state may possibly change). Alkaline-earth elements generally form permanently charged cationic species in solution which causes them to potentially accumulate in different locations, such as bone, compared to organics which are more likely to accumulate preferentially in soft tissue and fat (substitution for Calcium in the crystalline mineral component of bone matrix depending on such factors as the specificity of the cellular mechanisms involved in creation of bone mineral (e.g., osteoblast cation pumping proteins etc.) and the general physicochemical properties of the cation relative to Ca^{2+}). Perhaps even more so then than other bone seeking agents, which are more likely to be incorporated into bone matrix by adsorption to the surface and subsequent trapping, the dynamics of bone remodelling are of particular importance for the disposition of bone seeking cations such as Sr^{2+} and this is reflected in the design of the models of O'Flaherty *et al.* where great emphasis is also placed on the need to account for the anatomical and physiological changes that are associated with growth and senescence, and how these influence the parameters of bone physiology and disposition. Such considerations however are potentially of more limited concern for Strontium being used for treatment of postmenopausal osteoporosis and in the modelling of data from studies on a shorter timescale than such changes noticeably occur.

Aims and Objectives

In this paper, we present a physiologically based pharmacokinetic (PBPK) model to describe the disposition of Strontium in the rat (dosed as its Ranelate salt) that builds upon the work of O'Flaherty *et al.* This work aims to provide a model that uses a greater degree of physiological and mechanistic rationale than previously published, more empirical models used to describe the pharmacokinetics of Strontium (28–30), with particular focus on a detailed description of distributional processes in bone.

PBPK models are generally operated in either a closed or an open loop configuration for simulation and parameter estimation purposes. In a closed loop configuration the entire system of differential equations comprising the PBPK model is solved simultaneously, retaining the interdependence between individual tissues within the constraint of the mass-balance of the entire system. In an open loop configuration the closed circulation of the PBPK system is broken at the (arterial) blood compartment. The (arterial) blood concentration is fitted with an empirical PK model which is then used as a forcing function to describe the input concentration for the tissue compartments, the mass balance equations for which are solved independently and in parallel. Open loop PBPK modelling has advantages in that it is computationally and mathematically simpler to implement and that tissues that have no observations can be excluded from the model, however the open loop approach has the disadvantage that it does not retain the constraint of mass-balance on the overall model as each tissue is in effect treated separately. A secondary aim of the work in this paper is to investigate the performance of the PBPK model for Strontium disposition in both open and closed loop configurations to confirm that both perform similarly and that an open loop implementation of the model would be adequate for future applications.

MATERIALS AND METHODS

Animal Studies

Animal studies and sample analyses were carried out according to the principles of Good Laboratory Practice, at facilities of Servier research and development in the years 2000 to 2003, and in accordance with local ethical approval requirements and Principles of Laboratory Animal Care. Data was made available from the Servier archive for analysis and model development; the authors had no direct involvement in the design or execution of the *in-vivo* studies.

Strontium was quantified in plasma, by inductively coupled plasma atomic emission spectrometry (ICP-AES) at concentrations ranging from an LLOQ 0.0125 μg/ml up to 37 μg/ml; the precision (%CV) of the analytical method was between 2.3 and 6.7% with accuracy within 0.70% at the lowest QC concentration and within −0.30 to 3.2% of the target QC value at other concentrations. In bone, Strontium was quantified by inductively coupled plasma optical emission spectrometry (ICP-OES) following calcination and acid digestion of the dried bone samples; the

precision of the analytical method (%CV) was <5.3% with accuracy ranging between −0.9 to 1.5%. The bone assay LLOQ was 0.01 ug/ml with exposure in bone samples converted to mg/g of ash based on sample mass. Other tissue samples were analysed by laser ablation coupled with inductively coupled plasma mass spectrometry (LA-ICP-MS). The working range of the tissue sample assay was from an LLOQ of 1.5 µg Strontium/g tissue up to 500 µg/g; the mean intra-assay precision and accuracy of the analytical method was 7.2% and 4.4% respectively.

Ovariectomised (OVX) Female Rat Study (Parts I and II)

Ovariectomised (OVX) female rats are a preclinical disease model for post-menopausal osteoporosis, and plasma and bone exposure profiles were obtained for Strontium in a preclinical efficacy study in this model (with Strontium dosed as its Ranelate salt). Sprague Dawley rats aged ~28 weeks, were ovariectomised 9 weeks prior to the beginning of treatment to induce bone depletion. Part I of the study then involved PO dosing of subject animals at 250 mg/kg Strontium Ranelate (equivalent to 87.5 mg/kg active Strontium) once daily (QD) in a suspension dose form, for up to 6 months followed by a wash out period of a further 6 months. Three to four plasma samples were taken per animal over the timecourse with terminal sampling of bone tissue from three sites (L3-L4 vertebrae, femur and tibia). Samples were taken at time-points on day 1, and in weeks 1, 2, 4, 8, 16 and 26 during the treatment phase and on weeks 27, 28, 30, 34, 42 and 52 during the treatment free phase and were spread across the animals (totalling $n=140$) in a matrix sampling design to allow a composite profile to be constructed over the 12-month study period. The study also included a satellite IV PK study (part II), where $n=15$ subject animals were dosed with the equivalent of 8.29 mg/kg active Strontium (made up from the Strontium Chloride salt, and equivalent overall to 24 mg/kg Strontium Ranelate). This dose was administered over a 10 min IV infusion and 3–4 plasma samples (including a terminal sample) taken per subject, with time-points taken pre-dose and at 0.167 h during the infusion and then at 0.083, 0.167, 0.5, 1, 2, 3, 6, 8, 12, 24, 36, and 48 h post infusion. Samples were spread across individuals in a matrix sampling design to generate a composite profile over the 48 h study period.

Rat Tissue Exposure Study

Strontium tissue exposures were obtained from a rat tissue exposure study where subject animals were dosed PO at 250 mg/kg QD for 8 weeks, after which terminal blood and tissue samples were taken in separate groups at 2 h, 1 day, 1 week, 4 weeks and 8 weeks after the final dose ($n=3$ per time-point). Exposures from these samples are shown in Table VII (appendix 1), where it can be seen that by 1 week after the final dose, samples from all tissues apart from bone and teeth are BLQ. In the absence of other more suitable data, and given the inapplicability of in-silico partition coefficient (Kp) prediction methods given the physicochemistry of Strontium, the 2 h post dose samples from this study have been taken as the best approximation available to observed steady state tissue concentrations, and therefore blood to tissue ratios at 2 h have been used as an estimate of tissue partitioning for incorporation into a PBPK model as Kps.

Endogenous Baseline Strontium Measurement

In a limited number of subject animals in the datasets above predose plasma and bone samples were taken which on analysis revealed a small but consistent endogenous Strontium concentration. For plasma this was 0.015 mg/L (CV 10%) and bone 0.07 mg/g bone ash (CV 11%, average from all bone sites). Plasma and bone concentrations measured post dose were corrected by subtraction of this endogenous concentration. Where feasible this correction used the subject specific measurement of endogenous concentration, in animals where a predose was not taken the mean endogenous concentration was used. The baseline exposure levels observed are in keeping with the various assessments that exist in the literature regarding the endogenous levels of Strontium in plasma and bone (31–33).

Software

The PBPK model was implemented in Matlab (v 7.6.0, The Mathworks) as a system of ordinary differential equations, solved using the Matlab stiff numerical differential equation solver ode15s.

Model Structure and Equations

A schematic of the Strontium PBPK model structure is given in Fig. 1. An oral dose into the model enters the system *via* a first order absorption process (from a depot compartment representing the gut lumen) into the gut tissue compartment with the mass balance rate equation for the gut lumen expressing rate of change of *amount* in this compartment (Eq. 1). No further attempts to model absorption in a more mechanistic or physiological manner are made in the model and a fraction absorbed (F_{abs}) for a PO dose is incorporated *via* the initial condition applied in the gut depot compartment.

$$d\,A_{Gut\ Depot}/dt = -ka^{*}A_{Gut\ Depot} \quad (1)$$

Apart from the liver and kidney as eliminating organs, and the bone tissue compartments, tissues are modelled using perfusion limited PBPK tissue models (34) Tissues other than gut, lung, bone, kidney and liver are lumped into well-perfused (WP) and poorly-perfused (PP) tissue compartments. Mass balance rate equations for the *concentrations* of Strontium in the gut, lung, and the lumped tissue compartments are as follows (Eqs. 2 to 5), where Q is organ blood flow, Kp is the tissue:blood partition coefficient, and V is the organ volume. Blood recirculates in the model *via* the lung compartment and Q_{lung} is taken as cardiac output. $C_{Ven\text{-}blood}$ is the mixed venous concentration given by Eq. 14, and $C_{Art\text{-}blood}$ the arterial blood concentration given by Eq. 15.

$$\mathrm{d}\,C_{gut}/\mathrm{dt} = \left(ka * A_{Gut\ Depot} + Q_{gut} * C_{Art-blood} - Q_{gut} * C_{gut}/K_{P-gut}\right)/V_{gut} \quad (2)$$

$$\mathrm{d}\,C_{PP}/\mathrm{dt} = \left(Q_{PP} * C_{Art-blood} - Q_{PP} * C_{PP}/K_{P-PP}\right)/V_{PP} \quad (3)$$

$$\mathrm{d}\,C_{WP}/\mathrm{dt} = \left(Q_{WP} * C_{Art-blood} - Q_{WP} * C_{WP}/K_{P-WP}\right)/V_{WP} \quad (4)$$

$$\mathrm{d}\,C_{lungP}/\mathrm{dt} = \left(Q_{lung} * C_{Ven-blood} - Q_{lung} * C_{lungP}/K_{P-lung}\right)/V_{lung} \quad (5)$$

The kidney is modelled with a perfusion limited PBPK tissue model incorporating first order elimination, governed by CL_{renal} and fraction unbound in the kidney, (calculated from fraction unbound in blood (F_u) and the tissue Kp (Eq. 6).

$$\begin{aligned}\mathrm{d}\,C_{kidney}/\mathrm{dt} &= (Q_{kidney}{}^{*}C_{Art-blood} - Q_{kidney} * C_{kidney}/K_{P-kidney} \ldots \\ &\ldots - Cl_{renal} * C_{kidney} * F_u/K_{P-kidney})/V_{kidney}\end{aligned} \quad (6)$$

The liver accepts input blood flow not only from the arterial blood compartment, but also from the gut tissue *via* the hepatic portal vein, and is otherwise modelled like the kidney as a perfusion limited PBPK tissue model incorporating first order elimination, governed here however by the net hepato-biliary clearance $Cl_{hep\text{-}bil}$ and F_u (Eq. 7). Q_{liver} is taken as the sum of the physiological blood flows of the hepatic artery and the splanchnic tissues other than the gut—the splanchnic tissues are not explicitly included in the model and are assumed to account for a minimal part of the overall Strontium mass balance.

$$\begin{aligned}\mathrm{d}\,C_{liver}/\mathrm{dt} &= \left(Q_{liver}{}^{*}C_{Art-blood} + Q_{gut} * C_{gut}/K_{P-gut} \ldots\right. \\ &\ldots - \left(Q_{liver} + Q_{gut}\right) * C_{liver}/K_{P-liver} \ldots \\ &\ldots - Cl_{hep-bil} * C_{liver} * F_u/K_{P-liver}\left.\right)/V_{liver}\end{aligned} \quad (7)$$

Bone Tissue Modelling

Cortical and trabecular bone are assigned separate compartments within the model, and use a modification of the permeability rate limited tissue compartment model seen elsewhere in the PBPK literature (34). In this modification for bone tissue, the vascular compartment is taken as the bone surface and the extravascular the bone matrix, with exchange between the two governed by the processes of bone remodelling. The rate equations for the *amounts* in the surface and matrix compartments of trabecular and cortical bone take the same form (Eq. 8, where "x" may be substituted for "cortical" or "trabecular"):

$$\begin{aligned}\mathrm{d}A_{bone-surf-x}/\mathrm{dt} &= (Q_{bone-x} * C_{Art-blood}) \ldots \\ &-(Q_{bone-x} * A_{bone-surf-x}/(V_{bone-surf-x} * K_{P-bone-surf-x}) \ldots \\ &-(xRVAF * A_{bone-surf-x}/V_{bone-surf-x}) \ldots \\ &+(xBRR * A_{bone-matrix-x}/V_{bone-matrix-x}) \\ \mathrm{d}A_{bone-matrix-x}/\mathrm{dt} &= (xRVAF * A_{bone-surf-x}/V_{bone-surf-x}) \ldots \\ &-(xBRR * A_{bone-matrix-x}/V_{bone-matrix-x})\end{aligned} \quad (8)$$

The bone compartments describe solely the mineralised components of bone tissue, not soft tissue such as bone marrow which is incorporated into the lumped well perfused tissue compartment. The KP term for the vascularised bone surface acts to describe surface diffusion/adsorption onto the bone, while diffusion processes within the bone matrix itself are not reproduced in this model. In order to model the process of bone remodelling, the rates of bone formation and bone resorption are governed by the parameters "xRVAF" and "xBRR" which are calculated as follows by methods outlined by O'Flaherty *et al.* (35, 36). Fractional bone formation rate (FBFR) with units of h^{-1} is estimated *via* an allometric expression, dependent on the animal age in days (Eq. 9). FBFR is converted into a bone formation rate (BFR), with units of L/h by multiplying by the total volume of bone (Eq. 10). The overall rate of change of bone volume is assumed to be zero

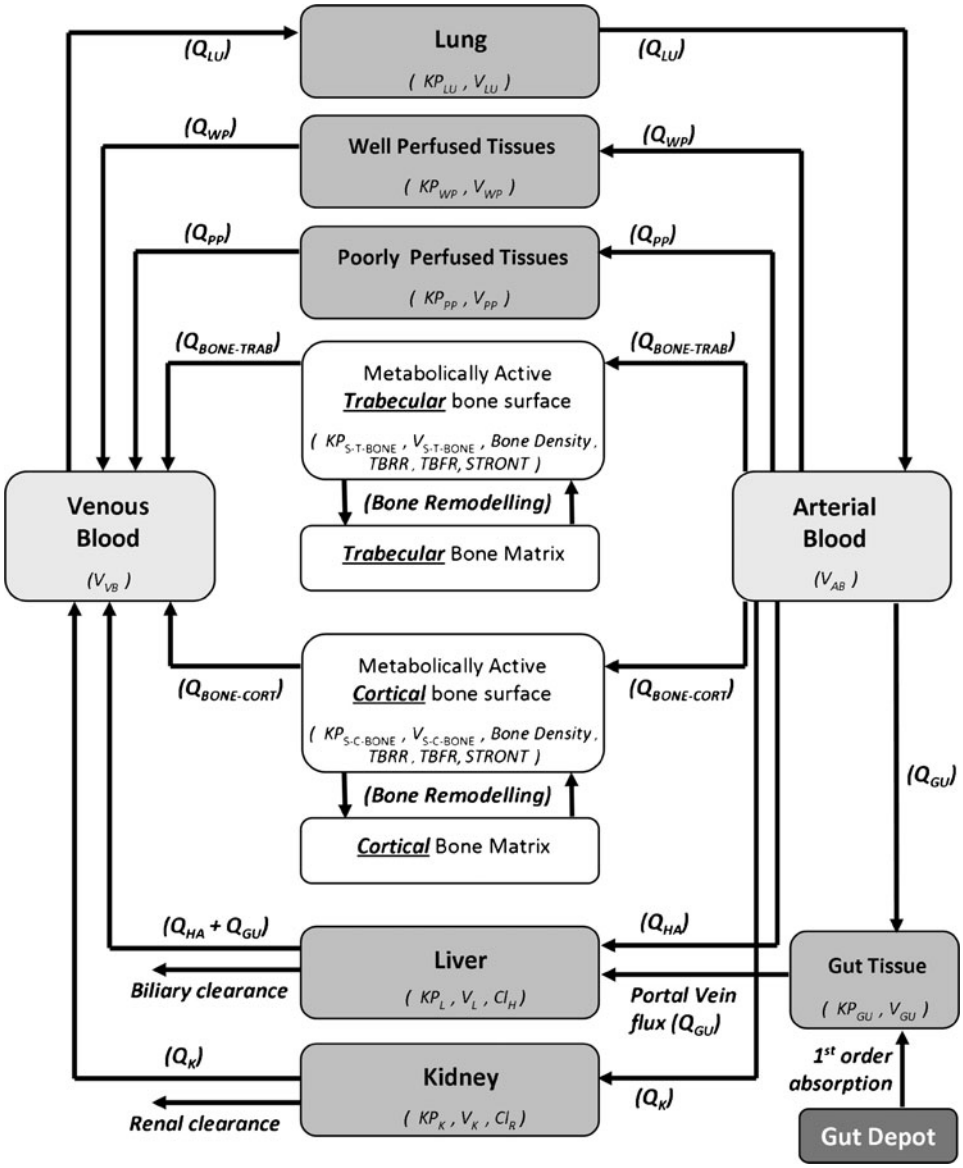

Fig. 1 Schematic of the PBPK model for Strontium.

over the timecourse of the study (i.e., there is no appreciable net bone growth) as the rats used in the study are mature adults; adult rats are known to continue to grow in size after reaching maturity (37) however the degree of change over the timecourse of this study is negligible. The bone resorption rate (BRR) can therefore be defined as being equal to the bone formation rate (Eq. 11).

$$\mathrm{FBFR} = (0.003 + 0.321^{*}\exp(-0.2^{*}\mathrm{AGE}) + 0.081^{*}\exp(-0.021^{*}\mathrm{AGE}))/24 \quad (9)$$

$$\mathrm{BFR} = \mathrm{FBFR}^{*}\mathrm{V_{bone}} \quad (10)$$

$$\mathrm{BRR} = \mathrm{BFR} \quad (11)$$

The equations above would allow bone formation and resorption rates to adopt separate values by allowing BRR to be defined as equal to BFR minus the overall rate of change of bone volume; this would be particularly important in the case of immature animals with a growing skeleton, where the rate of bone volume change would take a net positive value (with BFR greater in value than BRR). Once calculated, the BRR and BFR are partitioned into values for the separate trabecular and cortical bone compartments (TBFR, TBRR, CBFR and CBRR, with units of L/h) (Eq. 12).

$$\begin{aligned}\mathrm{TBFR} &= \mathrm{BFR}^{*}\mathrm{PART}\\ \mathrm{TBRR} &= \mathrm{BRR}^{*}\mathrm{PART}\\ \mathrm{CBFR} &= \mathrm{BFR}^{*}(1-\mathrm{PART})\\ \mathrm{CBRR} &= \mathrm{BRR}^{*}(1-\mathrm{PART})\end{aligned} \quad (12)$$

This calculation makes use of the constant "PART", equal to the *Fraction of total bone formation assigned to*

trabecular bone. A value for PART of 0.7 is assigned based on the higher surface area and blood flow of trabecular compared to cortical bone. It is largely constant between species that trabecular bone accounts for 67% of the total bone surface area and 63% of total bone blood flow (38). As the bone surface is the location of bone remodelling, trabecular bone is the region where the greater proportion of overall bone turnover will occur, which is in keeping with its generally more metabolically active status compared to cortical bone

The uptake/deposition of Strontium into the trabecular or cortical bone matrices from the surface compartment, due to bone formation is then described as an intercompartmental clearance (units of L/h), by scaling the bone formation rate in these compartments with the dimensionless scaling factor STRONT (Eq. 13).

$$\begin{aligned} \text{TRVAF} &= \text{STRONT}^{*}\text{TBFR} \\ \text{CRVAF} &= \text{STRONT}^{*}\text{CBFR} \end{aligned} \tag{13}$$

The use of the STRONT scaling parameter allows the rate of Strontium deposition into bone matrix to be governed by a rate parameter (xRVAF) of different value to that describing its release from bone matrix. This reflects that bone matrix formation/deposition is an active, ion-selective process governed by osteoblasts, while bone matrix resorption is of a less ion-selective nature governed by osteoclasts (using a combination of reduction in pH and proteases to dissolve and digest the mineral and proteinaceous components of the bone matrix, releasing the products into solution unselectively).

Equation 8 for the bone compartments has been left as describing amounts rather than converting them to concentrations. This is done out of convenience due to the way in which bone samples are taken, analysed and the exposure data reported. All bones contain a mixture of cortical and trabecular bone tissue according to their function, however when a bone sample is taken, no attempt will typically be made to separate out the cortical and trabecular bone tissue. In the case of the OVX rat data a whole femur for example (or tibia or vertebra) would be taken and treated (dried, calcinated, homogenised etc.) and analysed as a single sample despite the overall bone containing a mix of cortical and trabecular bone. Final exposure data is reported as the amount of Strontium per ash weight of bone. As a result what must be modelled to fit the data is neither the individual cortical or trabecular bone compartments but the *sum total of the amounts* in the two compartments, per the total ash weight of bone, as the amounts specifically in cortical or trabecular bone tissue (per the fractional ash weight of cortical or trabecular tissue respectively) are never reported. It might be thought then that the nature of the reported bone exposure data would make it better for the model to be reduced to having a single bone compartment, using combined physiological parameters for the two bone tissues. Such an approach however loses the more physiologically realistic description of the two very distinct bone tissue types—a well perfused, high surface area trabecular compartment with a lower physiological volume, and a less well perfused, lower surface area cortical compartment with a much larger physiological volume. Further, the model might lose the ability to describe a potentially multi-phasic overall bone profile that might result from the summation of two bone tissue compartments with very different individual PK profiles.

Table I Physiological Parameters Used in the Strontium PBPK Model

Parameter	units	value
weight	kg	0.380
AGE	days	196
Q_{gut} = blood flow to gut (portal vein)	L/h	0.591
Q_{PP} = blood flow to poorly perfused tissues	L/h	0.413
Q_{WP} = blood flow to well perfused tissues	L/h	2.624
Q_{lung} = blood flow to lung	L/h	4.399
Q_{kidney} = blood flow to kidney	L/h	0.552
Q_{liver} = blood flow to liver	L/h	0.160
$Q_{trab\text{-}bone}$ = blood flow to Trab. bone	L/h	0.062
$Q_{cort\text{-}bone}$ = blood flow to Cort. bone	L/h	0.037
V_{gut} = gut volume	L	0.011
V_{PP} = poorly perf. Tissues volume	L	0.270
V_{WP} = well perfused tissues volume	L	0.036
V_{lung} = lung volume	L	2.10×10^{-3}
V_{kidney} = kidney volume	L	3.70×10^{-3}
V_{liver} = liver volume	L	0.020
V_{BONE} = total bone volume	L	9.87×10^{-3}
$V_{BONE\text{-}SURF\text{-}TRAB}$ = Trabecular bone surface volume	L	3.95×10^{-5}
$V_{BONE\text{-}MATRIX\text{-}TRAB}$ = Trabecular bone matrix volume	L	1.93×10^{-3}
$V_{BONE\text{-}SURF\text{-}CORT}$ = Cortical bone surface volume	L	1.98×10^{-5}
$V_{BONE\text{-}SURF\text{-}CORT}$ = Cortical bone matrix volume	L	7.88×10^{-3}
$V_{ven\text{-}blood}$	L	0.017
$V_{art\text{-}blood}$	L	0.009
BONEWT = bone weight	g/100 g Body weight	5.00
BONEVOL = bone volume	mL/100 g Body weight	2.60
W_{BONE} = weight of marrow free dry bone	g	19
W_{ASH} = Ash weight of bone	g	10.716

Blood and Plasma Compartments

The mass balance rate equations for arterial and venous blood concentrations are defined in Eqs. 14 and 15. An auxiliary venous plasma compartment was modelled from the venous blood compartment (Eq. 16) for fitting to reported plasma exposure data by making use of the Strontium blood to plasma ratio (BPR).

$$\begin{aligned} dC_{Ven-blood}/dt &= \left((Q_{PP}{}^{*}C_{PP}/K_{P-PP}) + \left((Q_{WP}) * C_{WP}/K_{P-WP}\right)\right)\ldots \\ &+\left(Q_{kidney} * C_{kidney}/K_{P-kidney}\right)\ldots \\ &+\left(\left(Q_{liver} + Q_{gut}\right) * C_{liver}/K_{P=liver}\right)\ldots \\ &+\left(Q_{bone-\ trab} * A_{bone-surf-trab}/(V_{bone-surf-trab} * K_{P-bone-surf-trab})\right)\ldots \\ &+\left(Q_{bone-cort} * A_{bone-surf-cort}/(V_{bone-surf-cort} * K_{Pbone-surf-cort})\right)\ldots \\ &-\left(Q_{lung} * C_{Ven-blood}\right)\Big)/V_{Ven-blood} \end{aligned} \tag{14}$$

$$\begin{aligned} dC_{Art-blood}/dt &= \left(\left(Q_{lung} * C_{lung}\right)/K_{P-lung}\ldots\right. \\ &-\left(C_{Art-blood} * \left(Q_{PP} + Q_{WP} + Q_{kidney} + Q_{liver} + Q_{gut}\right)\right)\ldots \\ &\left.-\left(C_{Art-blood} * (Q_{bone-trab} + Q_{bone-cort})\right)\right)/V_{Art-blood} \end{aligned} \tag{15}$$

$$dC_{Ven-plasma}/dt = (dC_{Ven-blood}/dt)/BPR. \tag{16}$$

Finally, not illustrated in the model schematic is an extra compartment receiving the Strontium excreted by the liver and kidney, which was incorporated to allow calculation of the mass balance of the system as a diagnostic check that the model was performing correctly.

Model Parameters I: System Specific, Physiological Rat Parameters

A table of the physiological parameters that were used to implement the model and their values in the rat is presented in Table I.

Age and weight are the average values for the rats in the OVX rat dataset. Over the course of the OVX rat study the average weight of the subject animals increased from 368 to 430 g, a 16% gain converting to a rate of body weight change of 7×10^{-6}kg/h. This is in keeping with the known phenomenon of adult rats continuing to grow in size after reaching maturity (37) Various allometric equations exist to describe how organ sizes and other physiological parameters change in concordance with overall increase in body size, however, given that the rate of body weight change is small, these extra allometric relationships were not incorporated in the current model

Parameters Q_{liver}, Q_{gut}, Q_{kidney}, V_{liver}, V_{kidney}, V_{gut}, V_{lung} are all taken from Davies *et al.* (39). From the same reference, cardiac output in rats of approximately the size used in the current study is ~4.4 L/h and this was taken as the value for Q_{lung}. Total blood volume was taken from Davies *et al.* while the proportions accounted for by the venous and arterial blood pools was taken from Jones *et al.* (40), with venous and arterial blood accounting for 67% and 37% of total blood volume respectively.

Bone physiological parameters were taken or derived from constants described by O'Flaherty *et al.* (35). Total bone volume (V_{BONE}) was calculated as 2.6 mL per 100 g body weight. Based on a marrow free dry bone density of 1.92 g/mL, the ash weight of bone (W_{ASH}) was calculated as 0.564 times total marrow free dry bone weight. Total trabecular bone and total cortical bone volumes (i.e., surface+matrix components) were taken as 20 and 80% of total bone volume respectively. The specific surface and matrix volume fractions of the two compartments have been calculated to reflect the different surface area to volume ratios of the two types of bone tissue. Trabecular bone has a surface area to volume ratio of 20 mm^2 per mm^3 of bone while that of Cortical bone is 2.5 mm^2 per mm^3 of bone (26), leading to the calculations in Eqs. 17 and 18:

$$\begin{aligned} &\text{Trabecular bone surface area} = 20\ mm^2 \text{ per } mm^3 \text{ of bone} \\ &20\ mm^2/mm^3 = (20\times10^6)mm^2/(1\times10^6)mm^3 \\ &1\ dm^2 = 10^4 mm^2, (1\times10^6)mm^3 = 1\ dm^3 = 1 \text{ litre.} \\ &\text{Therefore :} \\ &2000\ dm^2/dm^3 = 2000\ dm^2/\text{litre} \\ &\text{Assuming the depth of the surface compartment is } 1\mu m = \\ &1*10^{-5}dm \\ &\text{Volume fraction}_{-BONE-SURF-TRAB} = \\ &(2000*10^{-5})\text{litre/litre bone} = 0.02 \\ &\text{Volume fraction}_{-BONE-MATRIX-TRAB} = 0.98 \\ &V_{BONE-TRAB-TOTAL} = 0.2 * V_{BONE}. \\ &\text{Therefore :} \\ &V_{-BONE-SURF-TRAB} = 3.95*10^{-5}L \\ &V_{-BONE-MATRIX-TRAB} = 1.93*10^{-3}L \end{aligned} \tag{17}$$

$$\begin{aligned} &\text{Cortical bone surface area} = 2.5\ mm^2 \text{ per } mm^3 \text{ of bone} \\ &\text{By the same method as Equation 17,} \\ &\text{Volume fraction}_{-BONE-SURF-CORT} = 0.0025 \\ &\text{Volume fraction}_{-BONE-MATRIX-CORT} = 0.9975 \\ &V_{BONE-CORT-TOTAL} = 0.8 * V_{BONE}. \text{ Therefore :} \\ &V_{-BONE-SURF-CORT} = 1.98*10^{-5}L \\ &V_{-BONE-MATRIX-CORT} = 0.0079\ L \end{aligned} \tag{18}$$

Q_{bone} and the fractions assigned to cortical and trabecular bone were all taken from O'Flaherty *et al.* (35) with trabecular bone accounting for 63% of total bone blood flow, and cortical bone the remaining 37%.

The volume of the well perfused rest of body compartment (V_{WP}) has been taken by O'Flaherty *et al.* as 10% of body weight assuming an average density of 1 kg/L, in a model lacking a specific lung compartment (36); V_{WP} is therefore calculated here as 10% of body weight *minus* V_{lung}. The volume of the poorly perfused rest of body compartment (V_{PP}) is calculated by subtraction from total body volume of all other tissue volumes.

Once the blood flows of the organs above have been taken into account, 3.0 L/h (68% of the total output) remains to be accounted for by the well perfused and poorly perfused rest of body tissue compartments. This has been partitioned as the well perfused compartment receiving 59% of cardiac output, and poorly perfused 9%, based on fractional tissue cardiac outputs as outlined by Brown *et al.* (41) and with Q_{PP} recalculated by subtraction of all other blood flows from cardiac output.

Model Parameters II: Strontium Specific Parameters and Optimised Parameters

The Strontium specific parameters used in the implementation of the O'Flaherty model are summarised in Table II.

Blood to plasma ratio, and fraction unbound in blood were determined for Strontium as part of internal experiments at Servier during drug development. Kp values for lung, liver, and kidney have been taken from the rat tissue distribution study described previously (see appendix 1 (Table VIII) for a full table of tissue:blood ratios derived from this study). The Kp values for lumped well perfused and poorly perfused tissues were calculated using the formula from Nestorov *et al.* (42) (Eq. 19). $Kp\text{-}_{WP}$ was calculated using the individual Kp values for brain, heart, and spleen, while $Kp\text{-}_{PP}$ used fat and skeletal muscle values. Clearly these individual organs cannot account for the entire well and poorly perfused rest of body compartments, but in the absence of Kp and/or blood flow information for other organs, and the inapplicability of Kp prediction methodologies given Strontium physicochemistry, the assumption was made to use the lumped Kp for the entire compartment. In the absence of any other available data, Kp-gut was given the same value as $Kp\text{-}_{WP}$.

$$K_{p\ lumped} = \frac{\sum_{i=1}^{n} Kp_i * V_i}{\sum_{i=1}^{n} V_i} \quad (19)$$

Fraction absorbed (F_a) was calculated as part of the empirical model fitting to the IV and PO plasma PK data carried out to enable the open loop configuration PBPK model fitting (see below).

Parameter Estimation

Fittings of the PBPK model to the available PK exposure data to estimate specific model parameters used the Matlab nonlinear least squares optimisation function LSQNONLIN, using objective functions weighted by $1/(\text{predicted value})^2$. Standard errors of parameter estimates were calculated using the method outlined by Landaw *et al.* (43) with the Jacobian of model parameter sensitivities estimated using a numerical central difference method. PK datasets comprised from multiple individual subject animals were treated as a naïve pool for data analysis purposes (44) rather than averaging the data at each time-point to create an "average rat" profile.

Open Loop Configuration Fitting

In open loop configuration only the bone tissue compartments were modelled as bone is the key tissue of interest and the only tissue other than blood for which a timecourse of Strontium measurements was available for optimising parameters and assessing model performance. In open loop configuration, Eq. 8 describing the bone compartments was used as written above, only with the input arterial blood concentration now provided by the central, blood describing compartment of an empirical PK model using the appropriate PO dosing regimen, with parameters estimated from an independent fitting made to the Strontium plasma PK profiles from the satellite IV PK study and the PO OVX rat study (also incorporating the blood to plasma ratio and with the assumption made that there is minimal difference in arterial and venous exposure). In this empirical analysis of the plasma data, the IV and PO profiles were analysed simultaneously (allowing for estimation of absolute bioavailability) and preliminary work revealed that an empirical 3-compartment, mammillary PK disposition model, with 1st order absorption for the PO data, (45), provided the most adequate fit to the plasma PK data. In the open loop configuration fitting of the bone tissue model to the observed Strontium bone exposure data from the OVX rat study, the Strontium specific parameters optimised were: STRONT, $Kp\text{-}_{BONE\text{-}SURF\text{-}TRAB}$ and $Kp\text{-}_{BONE\text{-}SURF\text{-}CORT}$. The modelled sum of the amount of Strontium in the trabecular and cortical bone compartments, normalised to the ash weight of bone, was fitted to the bone exposure profile provided by the mean bone exposures from the 3

Table II Strontium-specific, Un-optimised Parameters Used in the Strontium PBPK Model

Parameter	units	value
BPR = Sr blood to plasma ratio	n/a	0.48
F_U = fraction unbound in blood	n/a	0.73
Kp-lung = lung partition coeff	n/a	0.76
Kp_{liver} = liver partition coeff	n/a	0.47
Kp_{kidney} = kidney partition coeff	n/a	3.0
Kp_{gut} = gut tissue partition coeff	n/a	0.9
Kp_{-WP} = well perf tissue partition coeff	n/a	0.9
Kp_{-PP} = poorly perf tissue partition coeff	n/a	0.6
Fa = fraction absorbed	n/a	0.184

sites where bone was sampled (L3-L4 vertebrae, femur and tibia) in mg/g ash bone. Initial estimates for parameters during the nonlinear regression procedure were chosen *via* trial and error.

Closed Loop Configuration Fitting

For the closed loop configuration fitting, five Strontium specific parameters were optimised: Cl_{tot}, k_a, STRONT, $K_{P\text{-}BONE\text{-}SURF\text{-}TRAB}$ and $K_{P\text{-}BONE\text{-}SURF\text{-}CORT}$. The venous plasma compartment of the complete PBPK model was fitted to the observed PO plasma concentration data from the OVX rat study with simultaneous fitting of the modelled sum of the amount of Strontium in the trabecular and cortical bone compartments to the observed average bone-site exposure profile from the same study. IV plasma data was not required or used in this fitting and the assumption is made that there is negligible difference between the measured peripheral venous Strontium concentration and the modelled central mixed venous concentration. Initial estimates for parameters during the nonlinear regression were taken from the final estimates from the open loop fitting.

A quantitative breakdown of the routes of clearance for Strontium, giving a definitive proportion of total clearance accounted for by each, is not readily available in the literature for any species. The closest relevant studies in the rat (46, 47) only explicitly quantify Cl_{renal} and suggest this accounts for ~50% of total Strontium clearance in rat. It remains unclear therefore how the remainder of total Strontium clearance may be precisely accounted for by other routes. As a result, rather than try to attempt to incorporate all the other potential routes of clearance into this PBPK model (e.g., sweat, salivary secretion), the decision was taken to incorporate only renal and hepato-biliary excretion routes; the nominal hepato-biliary clearance will then account for all the non-renal routes of clearance. There is also potential for reabsorption of Strontium excreted in the bile, leading to enterohepatic recirculation; true net

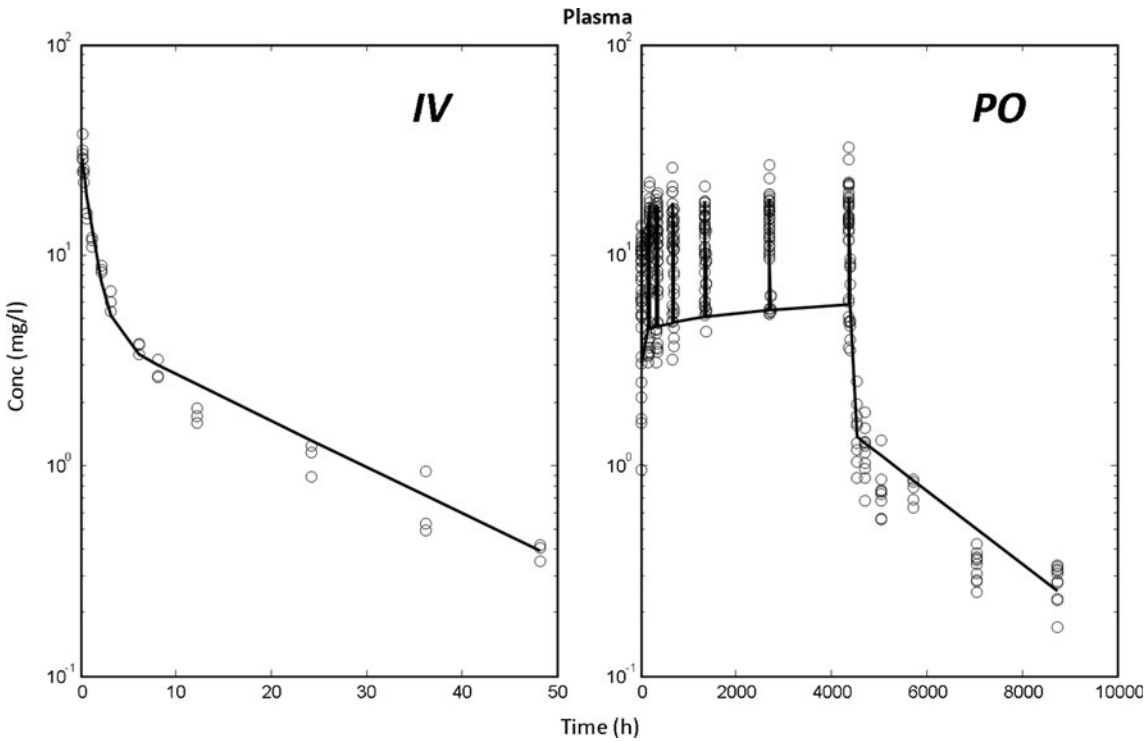

Fig. 2 Observed (*open circle symbols*) and Predicted (*solid line*) profiles from the 3 compartment empirical model fitting to IV and PO dosed rat Strontium plasma exposure data.

Table III Parameter Estimates (Est.), Standard Errors (se) and Relative Standard Errors Expressed as Coefficients of Variation (%CVs) for Mammillary 3-compartment, Empirical Model Nonlinear Least Squares Fitting to Naïve Pooled Rat Strontium Plasma IV and PO Profiles

	CL (L/h/kg)	Q2 (L/h/kg)	Q3 (L/h/kg)	V1 (L/kg)	V2 (L/kg)	V3-V2 (L/kg)	k_a (h^{-1})	F
Est.	0.061	0.155	0.011	0.269	0.825	22.826	0.308	0.184
se	0.003	0.0158	0.001	0.021	0.055	1.441	0.026	0.008
%CV	4.1	10.2	5.3	7.8	6.7	6.3	8.3	4.3

elimination *via* the bile will therefore be a function of parameters describing not only the biliary clearance itself, but the fraction (re)absorbed and the rate of gut transit removing Strontium out of the gut lumen. To avoid over-complication, this recirculation has not been incorporated into the model, and a hepato-biliary clearance parameter that accounts for the net sum of these processes has been used instead.

In fitting the closed loop configuration model to the data therefore, CL_{tot} is taken as an input (and this was the parameter directly optimised during model fitting) while CL_{renal} and $CL_{hepato\text{-}biliary}$ were each calculated as 50% of CL_{tot} for use in their tissue compartment models. CL_{renal} and $CL_{hepato\text{-}biliary}$ are thus optimised indirectly.

RESULTS AND DISCUSSION

Open Loop Model Fitting

A plot of predicted profiles (overlaid on the raw data) from the fitting of the empirical, mammillary, 3 compartment PK disposition model fitting to the IV and PO rat plasma Strontium PK profiles is given in Fig. 2, with parameter estimates and relative standard errors expressed as %CVs given in Table III.

Using the parameter estimates from the empirical plasma PK fitting to describe a driving, input blood forcing function for the bone tissue compartments, parameter estimates and relative standard errors expressed as %CVs from the open loop PBPK model fitting to the OVX rat bone exposure data are given in Table IV, with a plot of the predicted total bone exposure profile overlaid with the observed raw data in Fig. 3.

Table IV Parameter Estimates (Est.), Standard Errors (se) and Relative Standard Errors Expressed as Coefficients of Variation (%CVs) for Open Loop PBPK Model Nonlinear Least Squares Fitting to Naïve Pooled Rat Strontium Bone Exposure Profiles

	STRONT	$K_{P\text{-}BONE\text{-}SURF\text{-}TRAB}$	$K_{P\text{-}BONE\text{-}SURF\text{-}CORT}$
Est.	0.075	32180	76662
se	0.009	2906	12553
%CV	12.4	9.0	16.4

Closed Loop Model Fitting

Plots of predicted profiles (overlaid on the raw data) from the fitting of the closed loop configuration PBPK model to the observed OVX rat PO plasma *and* bone exposure profiles are given in Fig. 4, with parameter estimates and relative standard errors expressed as %CVs given in Table V. Strontium concentrations in liver, kidney, and lung compartments predicted by the closed loop model (simulated at 2 h after the final dose under the regimen of the tissue distribution study, using the final parameter estimates and the dosing) are reported in Table VI.

Visual inspection of the observed and predicted profiles indicate that both the open and closed loop modelled fits to the bone exposure data are adequate. In addition the values

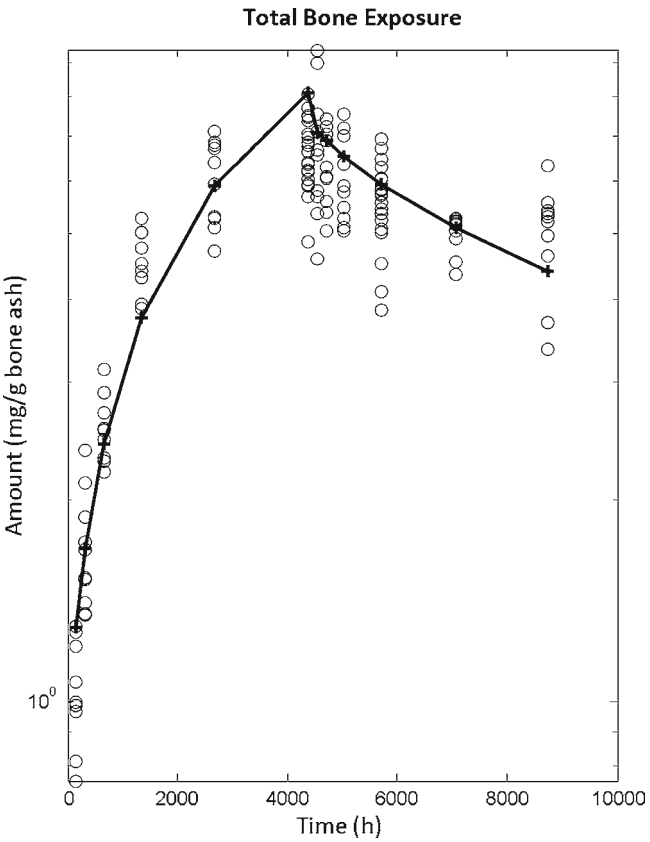

Fig. 3 Observed (*open circle symbols*) and predicted (*solid line*) total bone exposure profiles from the open loop PBPK model fitting to PO dosed rat Strontium bone exposure data.

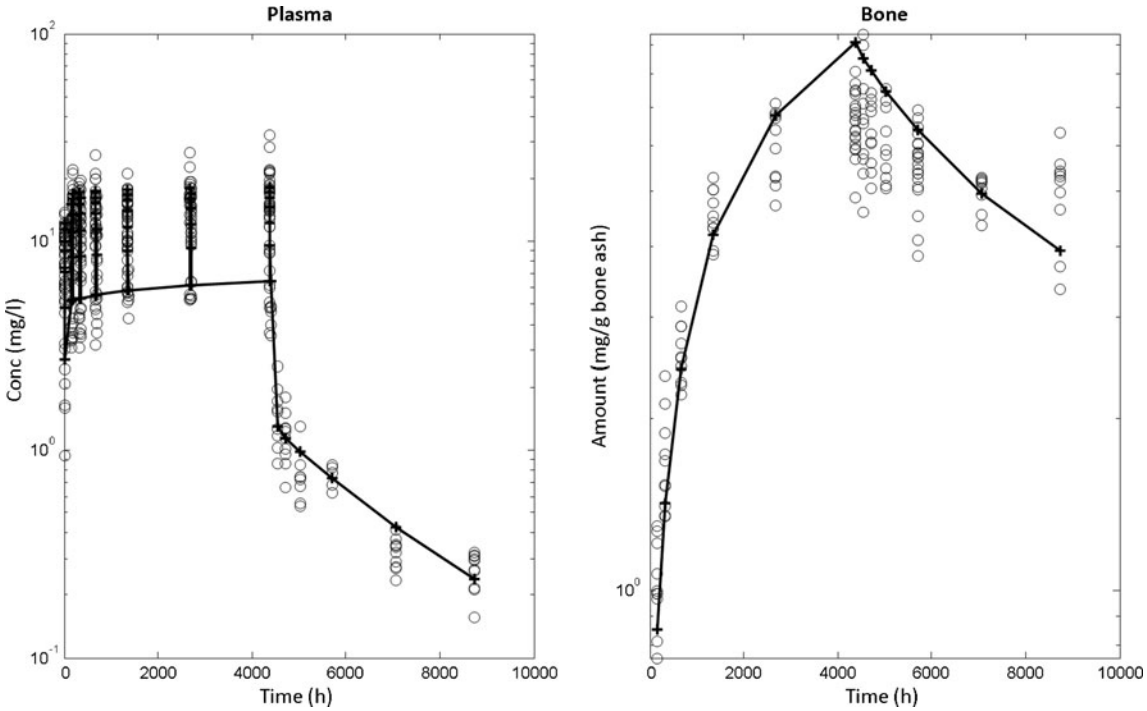

Fig. 4 Observed (*open circle symbols*) and predicted (*solid line*) plasma and total bone exposure profiles from the closed loop PBPK model fitting to PO dosed rat Strontium plasma and bone exposure data.

of the relative standard errors of the parameter estimates indicate the estimates are of acceptable quality given the dataset they have been derived from. The closed loop configuration model (having been fitted simultaneously to the plasma and bone exposure data) also provides an adequate description of the observed plasma exposure profile and predicts exposure levels in the liver, kidney and lung compartments that closely match observed values in these tissues. The description of the PO plasma profile by the closed loop model is of near identical quality to that seen by the fitting of a simple, empirical 3-compartment model to the same PO plasma data to facilitate the open loop implementation of the model (cf. Figs. 2 and 4). This is a further illustration that the PBPK model proposed is able to provide as equally good a description of the PK of Strontium as a simpler empirical model.

Table V Parameter Estimates (Est.), Standard Errors (se) and Relative Standard Errors Expressed as Coefficients of Variation (%CVs) for Closed Loop PBPK Model Nonlinear Least Squares Fitting to Naïve Pooled Rat Strontium Bone and Plasma Exposure Profiles

	Cl_{tot} (*L/h*)	k_a (h^{-1})	STRONT	$K_{P\text{-BONE-SURF-TRAB}}$	$K_{P\text{-BONE-SURF-CORT}}$
Est.	0.060	0.306	0.265	20481	17433
se	0.0009	0.013	0.027	1977	2107
%CV	1.4	4.5	10.1	9.7	12.1

The results show overall that the PBPK model is able to describe observed Strontium bone exposure within a physiologically rationalised framework beyond that utilised in previously published models of Strontium disposition (28) in both open and closed loop configurations. The estimated parameters that are held in common between the two configurations of the model (STRONT, $Kp_{\text{-bone-surf-trab}}$ and $Kp_{\text{-bone-surf-cort}}$) are of similar order of magnitude in the two fittings, with the high values of the estimated bone surface Kps reflecting the bone-seeking nature of Strontium.

Examining the predicted bone exposure profiles more closely, it is apparent that the closed loop configuration model tends to overpredict the bone exposure after dosing has ceased more than the open loop configuration model,

Table VI Observed and Predicted Tissue Concentrations in Specific, Non-lumped Model Tissue Compartments at 2 h Post Final Dose Under the Dose Regimen of the Rat Tissue Distribution Study (250 mg Sr Ranelate QD for 8 Weeks)

Tissue	Tissue exposure of Sr (ug/g) at 2 h post final dose after 8 weeks PO 250 mg/kg QD dosing (observed value mean $n = 3$)		
	Observed	Predicted	Fold diff in pred.
Kidney (mean of cortex and medulla)	19	24.5	1.3× over
Liver	3.1	4.4	1.4× over
Lung	5	6.5	1.3× over

though the overall fit of the two model configurations to the bone exposure profiles is similar. It is possible that this difference represents an artefact of the model fitting process where the closed loop fitting must optimise a set of parameters simultaneously describing the plasma and bone exposure profiles, while the open loop fitting only has to optimise parameters describing the bone profile and thus is able to achieve a closer fit to the bone profile alone. Examining the predicted profiles in the constituent trabecular and cortical bone tissue compartments (the sum of surface and matrix sub-compartments for each tissue sub-type) from the fittings in both configurations (Fig. 5) indicates that the two model configurations assign quite different proportions of the overall mass balance of Strontium to the two different bone tissue sub-types. As there is no definitive observation of the separate cortical and trabecular compartments, it is not possible to identify which configuration is more physiologically realistic, however in both configurations the higher remodelling rate of trabecular bone (with its richer blood supply, greater surface area and greater surface contact with bone marrow) is reflected in the steeper decline of the amount of Strontium in this compartment post dosing.

PBPK models have several advantages over their more empirical counterparts (34, 48). Where the data is available for their development as in this example with Strontium in the rat, a mechanistic PBPK model allows for a rationalised understanding of a drug's disposition based on physiological first principles that is not possible with a simpler empirical model. One of the more useful results that arises from such a mechanistic approach is the rational manner in which a PBPK model can allow for scaling to predict PK under different circumstances. If a PBPK model can be developed for a preclinical species as in this instance for Strontium, then it is relatively straightforward to derive a prediction of human PK by changing the physiological model parameters to their known values in human, (found e.g., in (39, 49, 50)) and drawing on other sources of information (or making appropriate assumptions or predictions) to assign values to the compound specific parameters. This may involve *in-vitro* experiments (e.g., protein binding), or optimisation through fitting the model to human exposure data, or assuming parameters take the same values as seen for the implementation of the model in rat. Once implemented, the human PBPK model can then be used as a rational means to predict human tissue concentrations, which is a further key advantage given that obtaining tissue samples from the majority of humans is typically difficult and limited. In the case of Strontium, where bone is the key tissue regarding its disposition and pharmacological efficacy this is particularly the case, increasing the potential value of a mechanistic PBPK model.

Having demonstrated the utility of this PBPK model with regard to describing Strontium disposition in the rat (in both

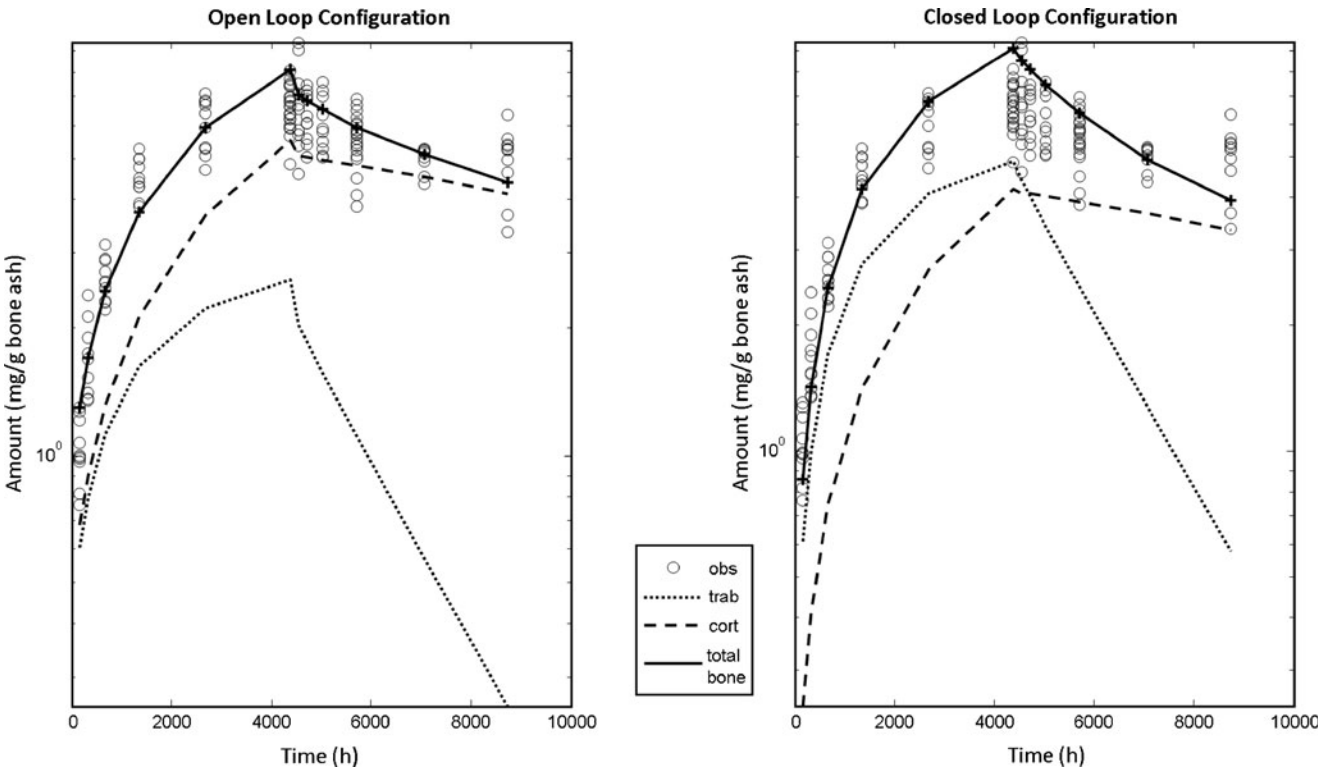

Fig. 5 Predicted total trabecular, total cortical and total sum of bone exposure profiles from closed and open loop PBPK model fittings to rat Strontium exposure data, overlaid with observed total bone exposure data.

open and closed loop configurations), various future applications of the model present themselves. The model may be applied for example to fitting observed Strontium PK exposure data using other statistical methods e.g., mixed effects, population based techniques looking to evaluate inter-individual variability in parameters across the observed population of subjects. In a population based statistical fitting paradigm the utility of the model in its less complicated open loop configuration has the advantage of reducing the numerical complexity of the structural model during the optimisation procedure.

The model may also be extended to allow a description of the pharmacodynamics (PD) of the pharmacological effect of Strontium on bone disposition. Strontium PK and PD will be very closely related as the key tissue for both its PK disposition and main PD effect is bone. The PBPK model for Strontium already includes mechanistic descriptions of the process of bone remodelling and turnover, so it should therefore be possible to incorporate a Strontium concentration dependent pharmacodynamic or efficacy component into the parameters governing the equations describing these processes (specifically the bone resorption and formation parameters BRR and BFR, as well as potentially making the bone volumes a time variant component of the model). These pharmacodynamic components might be able to make use of some of the mechanistic modelled descriptions of osteoblast/osteoclast activity that have already been outlined in the literature (51, 52). Scaling or further mathematical descriptors will then be necessary to relate these PD effects to biomarkers of outcome such as bone mineral density or biomarkers of bone turnover such as collagen CTX domain fragments etc. It may even be feasible to model an outcome biomarker such as bone fracture rate *via* some link to the bone mineral density (governed by the PK-PD of Strontium) and some form of time to event or hazard statistical model (in a similar way for example to the modelling conducted for the antiemetic pharmacodynamic response of Ondansetron (53)). There is also the possibility for interplay between the PK and PD effects to be described within the model in a manner similar to potential interactions seen for beta blockers or anaesthetics which can modulate hepatic blood flows and hence modulate their own pharmacokinetic behaviour. However, given that the model is able to achieve a reasonable description of the pharmacokinetic disposition of Strontium without explicit incorporation of its pharmacodynamic effect it would seem that (at least on the timescale of this particular study) that the net influence of feedback of the PD effect on the PK of Strontium is minor and that the degree of osteopenia/osteoporosis in the subject animals at the beginning of treatment was not drastic enough to effect the PK disposition of the bone tissue compartment.

Finally, it would also be feasible for the model to be applied to the description of the PK (and potentially PK-PD) of bone seeking agents other than Strontium by altering the Strontium specific parameters of the model as appropriate, while retaining the overall model structure and rationale.

CONCLUSION

In conclusion, a PBPK model has been developed that is able to describe plasma and bone exposure for Strontium in the OVX rat in a physiologically rationalised manner with parameter estimates and model behaviour in keeping with known aspects of the distribution and incorporation of Strontium into bone. The model has potential for future uses in modelling the PK-PD of Strontium and/or other bone seeking agents and for scaling to model human bone exposures for Strontium.

ACKNOWLEDGMENTS AND DISCLOSURES

The authors wish to thank Dr Kayode Ogungbenro and Dr Aris Dokoutmetzidis for their useful comments and assistance with Matlab during model development.

The authors would like also to acknowledge Dr Isabelle Dupin-Roger, Dr Pascal Delrat and Dr Emmanuelle Foos-Gilbert for their useful comments on Strontium pharmacology and Strontium ranelate pharmacokinetics in rat.

Work in this paper was funded by Servier research and development and by the School of Pharmacy and Pharmaceutical Sciences, The University of Manchester.

Part of this work was presented by the authors at the 20th Population Approach Group Europe (PAGE) meeting in Athens, Greece, June 7–10, 2011.

APPENDIX I

Tables of tissue concentrations and tissue-to-blood ratios from tissue distribution study.

Table VII Mean Strontium Tissue Concentrations Strontium Rat Tissue Distribution Study

Tissue		Mean ug/g in tissue ($n = 3$)				
		2 h	24 h	1 week	4 week	8 week
Heart Blood	Amt	6.6	BLQ	BLQ	BLQ	BLQ
	SD	4.3	NA	NA	NA	NA
	%RSD	66	NA	NA	NA	NA
Heart Muscle	Amt	8.4	BLQ	BLQ	BLQ	BLQ
	SD	4.2	NA	NA	NA	NA
	%RSD	50	NA	NA	NA	NA
Lung	Amt	5	BLQ	BLQ	BLQ	BLQ

Table VII (continued)

Tissue		Mean ug/g in tissue ($n = 3$)				
		2h	24h	1week	4week	8week
	SD	3	NA	NA	NA	NA
	%RSD	60	NA	NA	NA	NA
Liver	Amt	3.1	BLQ	BLQ	BLQ	BLQ
	SD	3.4	NA	NA	NA	NA
	%RSD	110	NA	NA	NA	NA
Brown Fat	Amt	13	BLQ	BLQ	BLQ	BLQ
	SD	7.5	NA	NA	NA	NA
	%RSD	58	NA	NA	NA	NA
Kidney Cortex	Amt	16	5.8	BLQ	BLQ	BLQ
	SD	5.9	3.3	NA	NA	NA
	%RSD	36	57	NA	NA	NA
Kidney Medulla	Amt	22	4.2	BLQ	BLQ	BLQ
	SD	15	2.4	NA	NA	NA
	%RSD	69	57	NA	NA	NA
Ovaries	Amt	44	4.2	BLQ	BLQ	BLQ
	SD	11	1.5	NA	NA	NA
	%RSD	24	37	NA	NA	NA
Spleen	Amt	7.3	BLQ	BLQ	BLQ	BLQ
	SD	3.4	NA	NA	NA	NA
	%RSD	47	NA	NA	NA	NA
Skeletal Muscle	Amt	3.8	BLQ	BLQ	BLQ	BLQ
	SD	2.6	NA	NA	NA	NA
	%RSD	70	NA	NA	NA	NA
Brain	Amt	1.5	2.3	BLQ	BLQ	BLQ
	SD	1.9	2.5	NA	NA	NA
	%RSD	129	108	NA	NA	NA
Lachrymal Gland	Amt	12	BLQ	BLQ	BLQ	BLQ
	SD	16	NA	NA	NA	NA
	%RSD	131	NA	NA	NA	NA
Thymus	Amt	2.8	BLQ	BLQ	BLQ	BLQ
	SD	2.6	NA	NA	NA	NA
	%RSD	93	NA	NA	NA	NA
Adrenal Gland	Amt	19	2.0	BLQ	BLQ	BLQ
	SD	5.8	1.5	NA	NA	NA
	%RSD	31	76	NA	NA	NA
Eye	Amt	BLQ	BLQ	BLQ	BLQ	BLQ
	SD	NA	NA	NA	NA	NA
	%RSD	NA	NA	NA	NA	NA
Uveal tract	Amt	25	1.9	BLQ	BLQ	BLQ
	SD	17	2.9	NA	NA	NA
	%RSD	67	158	NA	NA	NA
Spinal Cord	Amt	4	1.9	BLQ	BLQ	BLQ
	SD	3	1.7	NA	NA	NA
	%RSD	76	90	NA	NA	NA
Salivary Gland	Amt	11	12	BLQ	BLQ	BLQ
	SD	8.2	10	NA	NA	NA
	%RSD	72	87	NA	NA	NA

Table VII (continued)

Tissue		Mean ug/g in tissue ($n = 3$)				
		2h	24h	1week	4week	8week
Femur	Amt	2720	3390	2168	2895	1940
	SD	1036	1579	870	884	905
	%RSD	38	47	40	31	47
Vertebrae	Amt	4146	2803	2125	1943	1928
	SD	2589	1417	1112	1172	1222
	%RSD	63	51	52	60	63
Teeth	Amt	3598	2940	2787	1579	1295
	SD	784	1434	1428	1162	897
	%RSD	22	49	51	74	69

Table VIII Strontium Tissue to Blood Ratios at 2 h After Final Dose in Strontium Rat Tissue Distribution Study

Heart Blood	1	Lachrymal Gland	1.9
Heart Muscle	1.3	Thymus	0.42
Lung	0.76	Adrenal Gland	2.9
Liver	0.48	Eye	BLQ
Brown Fat	2	Uveal tract	3.8
Kidney Cortex	2.5	Spinal Cord	0.61
Kidney Medulla	3.3	Salivary Gland	1.8
Ovaries	6.7	Femur	415
Spleen	1.1	Vertebrae	632
Skeletal Muscle	0.57	Teeth	549
Brain	0.23		

REFERENCES

1. Shorr E, Carter AC. The usefulness of strontium as an adjuvant to calcium in the remineralization of the skeleton in man. Bull Hosp Joint Dis. 1952;13(1):59–66.
2. McCaslin FE, Janes HM. The effect of strontium lactate in the treatment of osteoporosis. Mayo Clin Proc. 1959;34:329–34.
3. An YH, RJ. F. Animal Models in Orthopaedic Research. Animal Models in Orthopaedic Research 1998.
4. Ammann P. Strontium ranelate: a physiological approach for an improved bone quality. Bone. 2006;38(2 Suppl 1):15–8.
5. Marie PJ, Hott M, Modrowski D, De Pollak C, Guillemain J, Deloffre P, *et al.* An uncoupling agent containing strontium prevents bone loss by depressing bone resorption and maintaining bone formation in estrogen-deficient rats. J Bone Miner Res. 1993;8(5):607–15.
6. Marie PJ, Ammann P, Boivin G, Rey C. Mechanisms of action and therapeutic potential of strontium in bone. Calcif Tissue Int. 2001;69(3):121–9.
7. Ammann P. Strontium ranelate: a novel mode of action leading to renewed bone quality. Osteoporos Int. 2005;16 Suppl 1:S11–5.

8. Marie PJ. Strontium ranelate: a novel mode of action optimizing bone formation and resorption. Osteoporos Int. 2005;16 Suppl 1:S7–S10.
9. Grynpas MD, Hamilton E, Cheung R, Tsouderos Y, Deloffre P, Hott M, *et al*. Strontium increases vertebral bone volume in rats at a low dose that does not induce detectable mineralization defect. Bone. 1996;18(3):253–9.
10. Busse B, Jobke B, Hahn M, Priemel M, Niecke M, Seitz S, *et al*. Effects of strontium ranelate administration on bisphosphonate-altered hydroxyapatite: Matrix incorporation of strontium is accompanied by changes in mineralization and microstructure. Acta Biomater. 2010;6(12):4513–21.
11. Jobke B, Burghardt AJ, Muche B, Hahn M, Semler J, Amling M, *et al*. Trabecular reorganization in consecutive iliac crest biopsies when switching from bisphosphonate to strontium ranelate treatment. PLoS One. 2011;6(8):e23638.
12. Canalis E, Hott M, Deloffre P, Tsouderos Y, Marie PJ. The divalent strontium salt S12911 enhances bone cell replication and bone formation *in vitro*. Bone. 1996;18(6):517–23.
13. Takahashi N, Sasaki T, Tsouderos Y, Suda T. S 12911–2 inhibits osteoclastic bone resorption *in vitro*. J Bone Miner Res. 2003;18(6):1082–7.
14. Meunier PJ, Roux C, Seeman E, Ortolani S, Badurski JE, Spector TD, *et al*. The effects of strontium ranelate on the risk of vertebral fracture in women with postmenopausal osteoporosis. N Engl J Med. 2004;350(5):459–68.
15. Reginster JY, Seeman E, De Vernejoul MC, Adami S, Compston J, Phenekos C, *et al*. Strontium ranelate reduces the risk of non-vertebral fractures in postmenopausal women with osteoporosis: Treatment of Peripheral Osteoporosis (TROPOS) study. J Clin Endocrinol Metab. 2005;90(5):2816–22.
16. Reginster JY, Kaufman JM, Goemaere S, Devogelaer JP, Benhamou CL, Felsenberg D, *et al*. Maintenance of antifracture efficacy over 10 years with strontium ranelate in postmenopausal osteoporosis. Osteoporos Int. 2011 Nov 29.
17. Stepensky D, Kleinberg L, Hoffman A. Bone as an effect compartment: models for uptake and release of drugs. Clin Pharmacokinet. 2003;42(10):863–81.
18. Pors NS. The biological role of strontium. Bone. 2004;35(3):583–8.
19. Dahl SG, Allain P, Marie PJ, Mauras Y, Boivin G, Ammann P, *et al*. Incorporation and distribution of strontium in bone. Bone. 2001;28(4):446–53.
20. Marie PJ. Strontium as therapy for osteoporosis. Curr Opin Pharmacol. 2005;5(6):633–6.
21. Apostoaei AI. Absorption of strontium from the gastrointestinal tract into plasma in healthy human adults. Health Phys. 2002;83(1):56–65.
22. Moraes ME, Aronson JK, Grahame-Smith DG. Intravenous strontium gluconate as a kinetic marker for calcium in healthy volunteers. Br J Clin Pharmacol. 1991;31(4):423–7.
23. Samachson J. The gastrointestinal clearance of Strontium-85 and calcium-45 in man. Radiat Res. 1966;27(1):64–74.
24. Samachson J, Spencer-Laszlo H. Urinary excretion of calcium and Strontium-85 in man. J Appl Phys. 1962;17:525–30.
25. Walser M. Renal Excretion of Alkaline Earths. In: Comar CL, Bronner F, editors. Mineral Metabolism. An Advanced Treatise. Chapter IV. New York: Academic; 1969. p. 235–320.
26. Mundy GR, Martin TJ. Physiology and pharmacology of bone. Physiology and pharmacology of bone: Handbook of experimental pharmacology; v 107. 1993:xxv, 762.
27. O'Flaherty EJ. Physiologically based models of metal kinetics. Crit Rev Toxicol. 1998;28(3):271–317.
28. Staub JF, Foos E, Courtin B, Jochemsen R, Perault-Staub AM. A nonlinear compartmental model of Sr metabolism. I. Non-steady-state kinetics and model building. Am J Physiol Regul Integr Comp Physiol. 2003;284(3):R819–34.
29. Staub JF, Foos E, Courtin B, Jochemsen R, Perault-Staub AM. A nonlinear compartmental model of Sr metabolism. II. Its physiological relevance for Ca metabolism. Am J Physiol Regul Integr Comp Physiol. 2003;284(3):R835–52.
30. Leggett RW. A generic age-specific biokinetic model for calcium-like elements. Radiat Prot Dosim. 1992;41(2–4):183–98.
31. Leeuwenkamp OR, van der Vijgh WJ, Husken BC, Lips P, Netelenbos JC. Quantification of strontium in plasma and urine with flameless atomic absorption spectrometry. Clin Chem. 1989;35(9):1911–4.
32. D'Haese PC, Van Landeghem GF, Lamberts LV, Bekaert VA, Schrooten I, De Broe ME. Measurement of strontium in serum, urine, bone, and soft tissues by Zeeman atomic absorption spectrometry. Clin Chem. 1997;43(1):121–8.
33. Barto R, Sips AJ, van der Vijgh WJ, Netelenbos JC. Sensitive method for analysis of strontium in human and animal plasma by graphite furnace atomic absorption spectrophotometry. Clin Chem. 1995;41(8 Pt 1):1159–63.
34. Nestorov I. Whole body pharmacokinetic models. Clin Pharmacokinet. 2003;42(10):883–908.
35. O'Flaherty EJ. Physiologically based models for bone-seeking elements. I. Rat skeletal and bone growth. Toxicol Appl Pharmacol. 1991;111(2):299–312.
36. O'Flaherty EJ. Physiologically based models for bone-seeking elements. II. Kinetics of lead disposition in rats. Toxicol Appl Pharmacol. 1991;111(2):313–31.
37. Zucker TF. The Growth Curve of the albino rat in relation to diet. J Nutr. 1941.
38. Mundy GR. Cellular and molecular regulation of bone turnover. Bone. 1999;24(5 Suppl):35S–8S.
39. Davies B, Morris T. Physiological parameters in laboratory animals and humans. Pharm Res. 1993;10(7):1093–5.
40. Jones HM, Parrott N, Jorga K, Lave T. A novel strategy for physiologically based predictions of human pharmacokinetics. Clin Pharmacokinet. 2006;45(5):511–42.
41. Brown RP, Delp MD, Lindstedt SL, Rhomberg LR, Beliles RP. Physiological parameter values for physiologically based pharmacokinetic models. Toxicol Ind Health. 1997;13(4):407–84.
42. Nestorov IA, Aarons LJ, Arundel PA, Rowland M. Lumping of whole-body physiologically based pharmacokinetic models. J Pharmacokinet Biopharm. 1998;26(1):21–46.
43. Landaw EM, DiStefano 3rd JJ. Multiexponential, multicompartmental, and noncompartmental modeling. II. Data analysis and statistical considerations. Am J Physiol. 1984;246(5 Pt 2):R665–77.
44. Ette EI, Williams PJ. Population pharmacokinetics II: estimation methods. Ann Pharmacother. 2004;38(11):1907–15.
45. Gibaldi M, Perrier D. Pharmacokinetics (2nd ed.). 1982.
46. Comar CL, Georgi J. Assessment of chronic exposure to radiostrontium by urinary assay. Nature. 1961;191:390–1.
47. Comar CL, Nold MM, Wasserman RH. Strontium-calcium discrimination factors in the rat. Proc Soc Exp Biol Med. 1956;92(4):859–63.
48. Aarons L. Physiologically based pharmacokinetic modelling: a sound mechanistic basis is needed. Br J Clin Pharmacol. 2005;60(6):581–3.
49. O'Flaherty EJ. Physiologically based models for bone-seeking elements. III. Human skeletal and bone growth. Toxicol Appl Pharmacol. 1991;111(2):332–41.

50. O'Flaherty EJ. Physiologically based models for bone-seeking elements. IV. Kinetics of lead disposition in humans. Toxicol Appl Pharmacol. 1993;118(1):16–29.
51. Lemaire V, Tobin FL, Greller LD, Cho CR, Suva LJ. Modeling the interactions between osteoblast and osteoclast activities in bone remodeling. J Theor Biol. 2004;229(3):293–309.
52. Bellido T, Ali AA, Plotkin LI, Fu Q, Gubrij I, Roberson PK, *et al.* Proteasomal degradation of Runx2 shortens parathyroid hormone-induced anti-apoptotic signaling in osteoblasts. A putative explanation for why intermittent administration is needed for bone anabolism. J Biol Chem. 2003;278(50):50259–72.
53. Cox EH, Veyrat-Follet C, Beal SL, Fuseau E, Kenkare S, Sheiner LB. A population pharmacokinetic-pharmacodynamic analysis of repeated measures time-to-event pharmacodynamic responses: the antiemetic effect of ondansetron. J Pharmacokinet Biopharm. 1999;27(6):625–44.